

Study of Lubricant Jet Flow Phenomena in Spur Gears – Out Of Mesh Condition *

D. P. Townsend† and L. S. Akin‡

In the lubrication and cooling of gears, the gear bulk temperature is an important component of the surface total temperature at the gear tooth contact point and thus is a controlling factor in the gear scoring or scuffing mode of surface failure. The method of applying the lubricant to the gears in most applications can have a large effect on the gear blank temperature. In reference 1 it was shown that scoring, which is a function of gear blank temperature, varies as a function of oil-jet velocity, direction, and location with regards to angular position from the gear mesh.

The depth of penetration of the oil jet into the gear blank also plays an important role in the gear blank temperature and, thus affects the scoring or scuffing limit of the gear. In references 2 and 3 the penetration depth for a jet pointed radially was determined for different gear conditions and lubricant drop sizes with windage effect included. It was assumed in those references that the radially pointed jet gives the best penetration depth and, therefore, the best gear cooling.

There are many gear applications where the oil jet is pointed at the mesh point and is either located into mesh (engaging) or out of mesh (disengaging). When the gear ratio is unity, the oil jet is usually pointed at the pitch point for in or out of mesh lubrication. However, when the gear ratio is different from unity, that is, when a speed increases or decreases, the jet may or may not be pointed at the pitch line. This could make considerable difference in the cooling of the gear or pinion and give unexpected results.

The objective of the work reported herein was to analytically and experimentally determine the penetration depth onto the tooth flank of a jet of oil at different velocities pointed at the pitch line on the outgoing side of mesh. The analysis determines the impingement depth for both the gear and the pinion. It includes the cases for speed increasers and decreasers as well as for one to one gear ratio. The work reported herein is an extension of the work reported in references 2 and 3 and is based on and extends the work reported in reference 4. In some cases the jet will strike the loaded side of the teeth, and in others it will strike the unloaded side of the teeth. In nearly all cases the top land will be cooled regardless of the penetration depth, and postimpingement oil spray will usually provide adequate amounts of oil for lubrication but is marginal or inadequate for cooling.

Symbols

B	gear or pinion backlash, m (in.)
H	impingement depth, m (in.)
h_k	whole depth, m (in.)
L	distance from line of centers to impingement point, m (in.)
m_g	gear ratio
N	number of teeth
n	rotational speed, rpm
P	module, (diametral pitch)
R	pinion radius, m (in.) ($2R = D$)
r	gear radius, m (in.)
t	time, sec
v	pitch line velocity, m/sec (in/sec)
v_j	jet velocity, m/sec (in/sec)
γ	dimensionless impingement depth

*Previously published in the January 1978 issue of ASME's Journal of Mechanical Design and as NASA TM-73694.

†NASA Lewis Research Center.

‡Western Gear Corporation, Lynnwood, California.

θ gear or pinion angle of rotation from line of centers, rad
 φ pressure angle, rad
 ω gear or pinion rotation speed, rad/sec

Subscripts:

b base circle
 g gear
 o outside radius
 p pinion

Test Apparatus

The lubricant oil jet tests were performed in the NASA Lewis gear test apparatus shown in figure 1 and described more fully in references 2 and 5. This test rig uses the four-square principle of loading the test gears. Load is applied to the gears by a hydraulic loading system.

The test gears were 8 diametral pitch, having a 8.89-cm (3.5-in.) pitch diameter, a 20° pressure angle, and a whole depth of 0.762 cm (0.300 in.). The gears were made with a very wide face width to allow for the coverage of light and oil spray for test conditions. The gear material was a low carbon steel.

A specially designed test gear cover was made for the lubrication tests. The cover has two windows, 90° apart, for admitting light to the test gears and a viewing window in front of the gears for viewing or photographing the lubrication phenomenon. The viewing window and the light windows are protected from oil splash by shielding. The windows are constantly swept by a thin film of high-velocity air blown across the windows to keep them free of oil for good light passage. V-jet, oil nozzles are located behind each of the light windows and spray a thin fan shaped stream of oil onto the gear teeth parallel to the gear axis. A 1000-V xenon lamp was used to illuminate the lubricant. The light from the xenon lamp is passed through a condenser lens to give a parallel light, it then passes through a cylindrical lens to bring the light into focus as a narrow slit. The light, which is reflected by a 45° mirror, passes through the light window and crosses the fanshaped oil stream.

The lubricant used in the tests was a clear mineral oil to which was added approximately 10 percent by volume white lithopone pigment, which gave it the appearance of milk. When the narrow band of intense light crossed the fan of white oil, a bright line of it was illuminated so that it could be

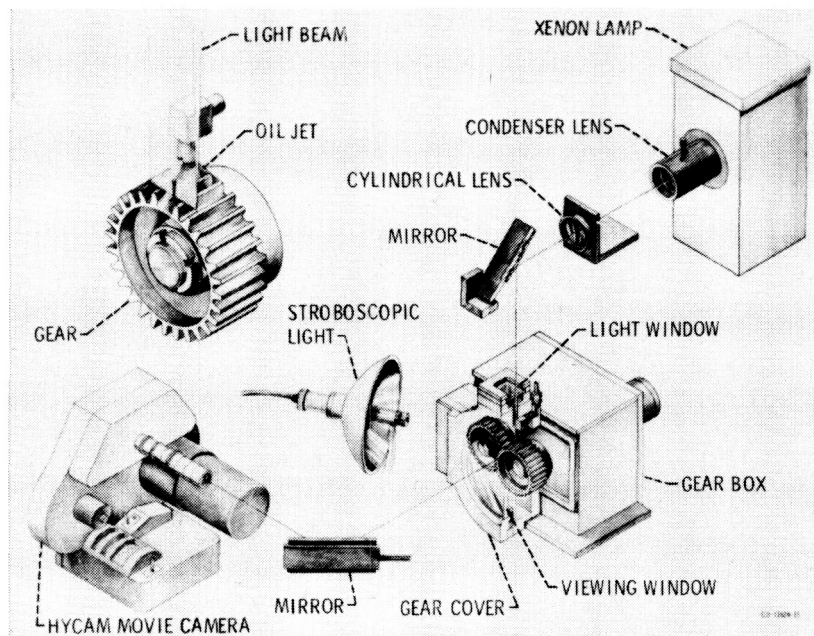


Figure 1. - Test setup for oil-jet penetration study.

photographed with a high-speed camera.

A high-speed Hycam movie camera was used to photograph the oil jet through a 45° mirror and the gearbox cover window. A high-speed, air-cooled stroboscopic system was used to provide flash-tube lighting that was synchronized with the high-speed camera. The camera speed was set to give a frame for each tooth space movement. The stroboscopic system had a timer that prevented burnout of the flash tube.

Analytical Approach – Disengaging Mesh

Impingement on Driving Pinion

As the oil jet approaches the tooth surfaces, it must first clear the gear tooth to approach the pinion; likewise, it must clear the pinion tooth to approach the gear tooth. In figure 2 the gear tooth is at the position where the oil jet starts to clear the gear tooth and move toward the pinion. The gear-tooth loaded-side pitch-point position at this instant ($t=0$), as measured from the line of centers is

$$\theta_{gl} = \cos^{-1} \frac{R}{R_o} - \text{inv } \varphi_{og} + \text{inv } \varphi \quad (1)$$

The corresponding pitch-point position on the pinion loaded side, which was in contact with the gear at the line of centers, is $m_g \theta_{gl}$. Therefore, the position of the pinion tooth at the base circle (point 2, fig. 2) at time ($t=0$) is

$$\theta_{pl} = m_g \left(\cos^{-1} \frac{R}{R_o} - \text{inv } \varphi_{og} + \text{inv } \varphi \right) + \text{inv } \varphi \quad (2)$$

As the jet goes from position 1 on the gear to position 4 on the pinion (as shown in fig. 3), the pinion is rotating through the angle $\theta_{p2} - \theta_{p1}$, or from position 2 to position 3 in figure 3. The time required for the pinion to get from point 2 to point 3 is

$$t_{2-3} = \frac{\theta_{p2} - \theta_{p1}}{\omega_p} \quad (3)$$

At the same time the oil jet with velocity v_o moves through the distance $(R_o^2 - R^2)^{1/2} - L_p$ (fig. 3) so that

$$t_{1-4} = \frac{(R_o^2 - R^2)^{1/2} - L_p}{v_j} \quad (4)$$

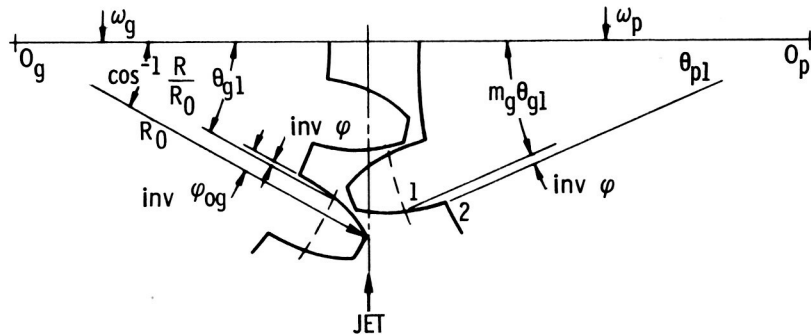


Figure 2

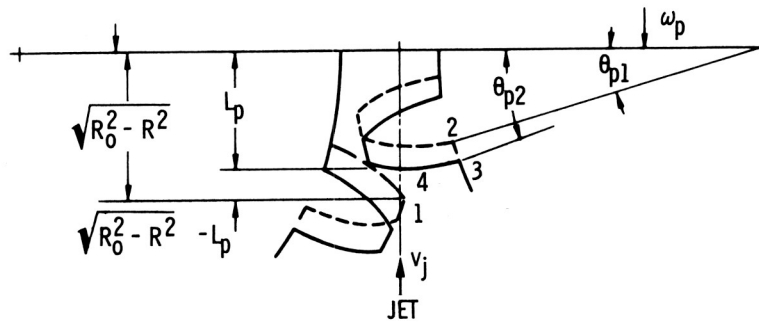


Figure 3

Since t_{2-3} must be equal to R_{1-4} then,

$$\frac{\theta_{p2} - \theta_{p1}}{\omega_p} = \frac{(R_0^2 - R^2)^{1/2} - L_p}{v_j} \quad (5)$$

Equation (5) cannot be solved for L_p , since θ_{p2} is also unknown. From figure 4 let

$$\theta_{p3} = \cos^{-1} \frac{r_b}{(r^2 + L_p^2)^{1/2}} \quad (6)$$

and

$$\theta_{p2} = \tan^{-1} \frac{L_p}{r} + \text{inv } \theta_{p3} \quad (7)$$

Substituting equation (7) into equation (5) and making use of equation (6) allows an implicit equation in L to be expressed in terms of time of flight by setting equations (3) and (4) equal, as

$$\frac{\tan^{-1} L_p/r + \text{inv } \theta_{p3} - \theta_{p1}}{\omega_p} = \frac{(R_0^2 - R^2)^{1/2} - L_p}{v_j} \quad (8)$$

Equation (8) can be solved iteratively for L_p . Once L_p is known, the impingement depth H_p (fig. 4)

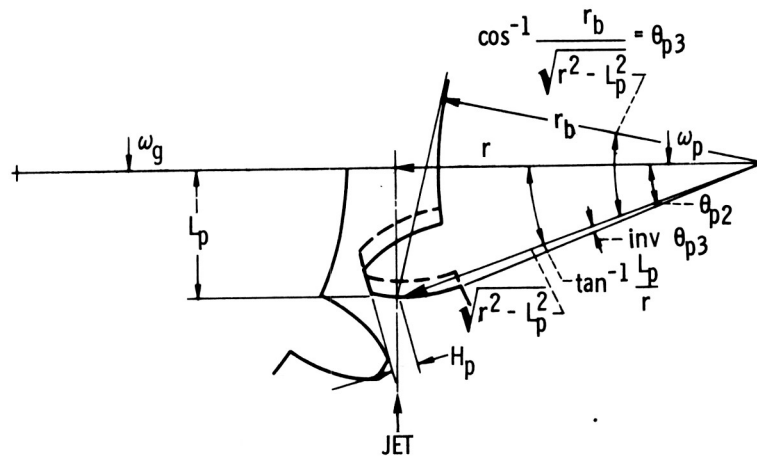


Figure 4

can be determined as

$$H_p = r_o - (R^2 + L_p^2)^{1/2} \quad (9)$$

The whole depth h_k may be used to normalize the impingement depth to its dimensionless form γ_p for a standard gear as

$$\gamma_p = \frac{H_p}{h_k} = \left[r_o - (r^2 - L_p^2)^{1/2} \right] \frac{P}{2} \quad (10)$$

It can be seen that the gear outside diameter crosses the jet line ahead of the pinion and is the initial shield for the pinion tooth. The same is true for the pinion outside diameter, which crosses the jet line ahead of the gear and is the initial shield for the gear tooth. However, at high gear ratios, it is possible for the gear to shield the pinion entirely so that the pinion would receive no cooling unless the jet direction and/or position is modified. The following three tests may be used to determine the condition for zero impingement depth on the pinion: when

$$\tan^{-1} \frac{L_p}{r} < \cos^{-1} \frac{r}{r_o}$$

or

$$L_p < (r_o^2 - r^2)^{1/2}$$

and when

$$h_p \leq 0$$

Impingement on Driven Pinion

As the oil jet clears the gear tooth (position 1 in fig. 5) and approaches the unloaded side of the pinion tooth at $t=0$, the position of the loaded-side gear tooth pitch point from the line of center is

$$\theta_{gl} = \cos^{-1} \frac{R}{R_o} - \text{inv } \varphi_{og} + \text{inv } \varphi - \frac{\pi}{N_g} - B_g \quad (11)$$

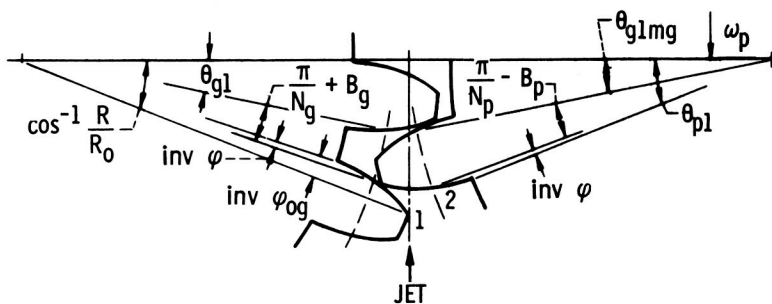


Figure 5

The corresponding pinion pitch-point position at $t=0$ on the pinion loaded side, assuming conjugate action, is $m_g \theta_{g1}$. Therefore, the position of the pinion tooth unloaded side at the base circle at $t=0$ is

$$\theta_{p1} = m_g \theta_{g1} + \frac{\pi}{N_p} - B_p + \text{inv } \varphi \quad (12)$$

The time it takes the jet to go from position 1 in figure 5 and impinge on the unloaded side of the pinion tooth t_{2-3} is equal to the time it takes the pinion to rotate from position 2 to position 3 in figure 3. Therefore, the relationships shown in figures 3 and 4 are valid for this case so that the time of flight is

$$\frac{\tan^{-1}(L_p/r) + \text{inv } \theta_{p3} - \theta_{p1}}{\omega_p} = \frac{(R_o^2 - R^2)^{1/2} - L_p}{v_j} \quad (13)$$

This is similar to the pinion-driving case, but it will have a slightly different value for L_p because of the B_p and B_g terms. The dimensionless impingement depth normalized by the whole depth is the same as for the driving pinion case and is expressed as

$$\gamma_p = \frac{H_p}{h_k} = \frac{r_o - (r^2 + L_p^2)^{1/2}}{P/2} \quad (14)$$

Impingement on Driving Gear

When the pinion outside diameter clears the oil jet at position 5 in figure 6, the jet approaches the loaded side of the gear tooth. The position of the pinion loaded-side pitch point from the line of centers at this time ($t=0$) is

$$\theta_{p4} = \cos^{-1} \frac{r}{r_o} - \text{inv } \varphi_{op} + \text{inv } \varphi \quad (15)$$

The position of the gear loaded-side pitch point from the line of centers is θ_{p4}/m_g and the gear-tooth loaded-side base circle point (as shown in fig. 6) is

$$\theta_{g2} = \frac{\theta_{p4}}{m_g} + \text{inv } \varphi \quad (16)$$

As the gear rotates through the angle $(\theta_{g3} - \theta_{g2})$; shown in fig. 7) from position 6 to position 7, the jet moves through the distance

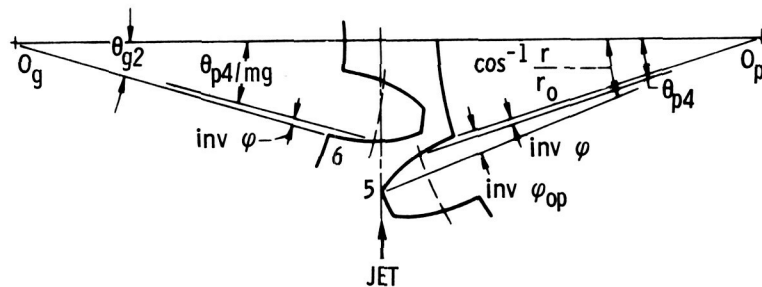


Figure 6

$$\theta_{g4} = \cos^{-1} \frac{R_b}{(R^2 + L_g^2)^{1/2}} \quad (20)$$

and

$$\theta_{g3} = \tan^{-1} \frac{L_g}{R} + \text{inv } \theta_{g4} \quad (21)$$

Substituting equation (21) into equation (19) and using equation (20) for θ_{g4} gives an implicit equation in L_g expressed as

$$\frac{\tan^{-1} L_g/R + \text{inv } \theta_{g4} - \theta_{g2}}{\omega_g} = \frac{(r_o^2 - r^2)^{1/2} - L_g}{v_j} \quad (22)$$

Equation (22) must be solved iteratively for L_g . The impingement depth H_g (fig. 8) can be expressed as

$$H_g = R_o - (R^2 - L_g^2)^{1/2} \quad (23)$$

Expressed in dimensionless depth in terms of the whole depth gives

$$\gamma_g = \frac{H_g}{h_k} = (R_o - \sqrt{R^2 - L_g^2}) \frac{P}{2} \quad (24)$$

Impingement on Driven Gear

As the outside diameter of the pinion tooth passes the jet at position 5 (fig. 9), the jet begins to approach the unloaded side of the gear tooth at time ($t=0$). The position of the loaded-side pinion pitch point from the line of centers at time ($t=0$), as shown in figure 9, is

$$\theta_{p4} = \cos^{-1} \frac{r}{r_o} - \text{inv } \varphi_{op} + \text{inv } \varphi - \frac{\pi}{N_p} - B_p \quad (25)$$

The corresponding position of the gear loaded-side pitch point is θ_{p4}/m_g . The position of the unloaded side of the gear tooth at time ($t=0$) at the base circle position 6 of figure 9 may be determined from

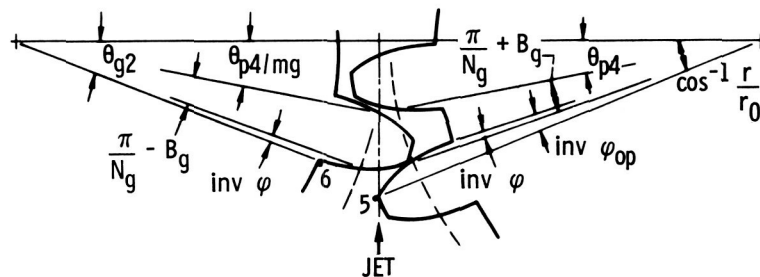


Figure 9

$$\theta_{g2} = \frac{\theta_{p4}}{m_g} + \frac{\pi}{N_g} - B_g + \text{inv } \varphi \quad (26)$$

The jet passes from position 5 to 8 while the gear rotates from position 6 to 7 (fig. 7). The time required for the gear to rotate from position 6 to 7 is

$$t_{6-7} = \frac{\theta_{g3} - \theta_{g2}}{\omega_g} \quad (27)$$

During this time the oil jet moves through the distance $(r_o^2 - r^2)^{1/2} - L_g$ and its time of flight over this distance is

$$t_{5-8} = \frac{(r_o^2 - r^2)^{1/2} - L_g}{v_j} \quad (28)$$

The gear rotation time t_{6-7} must be equal to the oil jet time of flight t_{5-8} so that

$$\frac{\theta_{g3} - \theta_{g2}}{\omega_g} = \frac{(r_o^2 - r^2)^{1/2} - L_g}{v_j} \quad (29)$$

From figure 8 it can be seen that

$$\theta_{g4} = \cos^{-1} \frac{R_b}{(R^2 + L_g^2)^{1/2}} \quad (30)$$

and

$$\theta_{g3} = \tan^{-1} \frac{L_g}{R} + \text{inv } \theta_{g4} \quad (31)$$

Substituting equation (31) into equation (29) and using equation (30) for θ_{g4} gives an implicit equation in terms of the time of flight as

$$\frac{\tan^{-1} L_g/R + \text{inv } \theta_{g4} - \theta_{g2}}{\omega_g} = \frac{(r_o^2 - r^2)^{1/2} - L_g}{v_j} \quad (32)$$

This equation must be solved iteratively for L_g . The impingement depth for the unloaded side of the gear (fig. 8) may now be determined as

$$H_g = R_o - (R^2 + L_g^2)^{1/2} \quad (33)$$

and the dimensionless impingement depth in terms of the whole depth may be written as

$$\gamma_g = \frac{H_g}{h_k} = R_o - \left[(R^2 + L_g^2)^{1/2} \right] \frac{P}{2} \quad (34)$$

This is the same as for the driving gear case except for the effects of backlash B_p and B_g .

Reduction of Impingement Depth by Gear Chopping

As the gear ratio is increased, the gear completely shields the pinion so that it no longer blocks the gear tooth. However, the impingement depth on the gear itself is reduced by chopping of the oil jet by the leading tooth. The pinion impingement depth can be improved by moving the jet in the direction of the pinion, but this does not improve the gear impingement depth. The gear impingement depth can be improved by pointing the jet toward the gear. Figures 2, 6, and 7 will be used again here to illustrate the mathematics of this portion of the operational problem.

When the gear ratio is sufficiently large, the leading gear tooth shields the trailing tooth instead of the pinion (similar to figure 2). The position of the back-side pitch point of the leading gear tooth from the line of centers at $t=0$ is (as shown similarly in fig. 2; no separate figure is provided.)

$$\theta_{g1} = \cos^{-1} \frac{R}{R_o} - \text{inv } \theta_{og} + \text{inv } \varphi \quad (35)$$

The trailing gear-tooth impingement-side base circle position from the line of centers at time ($t=0$) is θ_{g2} (shown in a similar position 6 in fig. 6 as θ_{g2}) and can be determined from the relations

$$\theta_{g2'} = \theta_{g1} - \frac{\pi}{N_g} + \text{inv } \varphi \quad (36)$$

and

$$\theta_{g2'} = \cos^{-1} \frac{R}{R_o} - \frac{\pi}{N_g} - \text{inv } \varphi_{og} + 2 \text{inv } \varphi \quad (37)$$

This bridging of the tooth space by the term π/N_g can be seen in figure 5, but the equations do not include a term for backlash B_g .

The time required for the gear to rotate at a speed ω_g from position 6 to 7 (fig. 7) is

$$t_{6-7} = \frac{\theta_{g3} - \theta_{g2'}}{\omega_g} \quad (38)$$

At the same time the oil jet travels from position 1 (fig. 3) to position 8 (fig. 7) at a speed of v_j and may be calculated as

$$t_{1-8} = \frac{(R_o^2 - R^2)^{1/2} - L_g}{v_j} \quad (39)$$

Using the geometry of figures 7 and 8, an equation may be written for gear rotation θ_{g3} in terms of L_g :

$$\theta_{g3} = \tan^{-1} \frac{L_g}{R} + \text{inv } \theta_{g4} \quad (40)$$

where

$$\theta_{g4} = \cos^{-1} \frac{R_b}{(R^2 + L_g^2)^{1/2}} \quad (41)$$

An expression can now be written for the time of flight in terms of L_g by setting the gear rotation t_{6-7} equal to the time of flight t_{1-8} and using equation (40) for θ_{g3} as follows:

$$t = \frac{\tan^{-1} L_g/R + \text{inv } \theta_{g4} - \theta_{g2}}{\omega_g} = \frac{(R_o^2 - R^2)^{1/2} - L_g}{v_j} \quad (42)$$

This implicit equation can be solved iteratively for L_g (fig. 8). From equation (42) the limiting value of H_g for gear chopping can be found and identified as H_g and will considerably limit the penetration depth (fig. 13).

Impingement On Engaging Side of Mesh

When the oil-jet velocity is equal to or exceeds the pitch-line velocity, the oil will impinge on the loaded side of one member and the unloaded side of the other. The amount of oil impinging on the pinion at high gear ratios will be small because of gear tooth chopping, and, at jet velocities exceeding the pitch-line velocity, the oil may never hit the pinion because of gear chopping. The pressure needed to provide oil at the pitch-line velocity is $7.8 \times 10^{-4} (C_v n D)^2$ Pa ($1.13 \times 10^{-7} (C_v n D)^2$ psi). Gear chopping on the out-of-mesh side will stop the oil jet, whereas on the into-mesh side it only interrupts the jet, letting the interrupted stream continue into mesh with the teeth. As can be seen in figure 10 the oil jet impinges on the gear profile starting at point 1 and continues uninterrupted until the pinion at point 4 or the following tooth at point 3 interrupts the jet stream. If the jet stream is at or near pitch-line velocity, it will continue to impinge on the tooth profile of either the gear or pinion until the pitch point. At slower velocities it will impinge on the side of the tooth opposite the jet. At higher velocities, it will have less impingement depth than at pitch-line velocity. The oil ahead of the contact point will be squeezed out, lubricating the full depth working surface. However, the contact point is where heating takes place, and, since there is only a very small amount of oil in the contact zone and remaining on the surface after contact, the effective cooling is very small for into-mesh lubrication. In addition, too much oil going into mesh will cause the teeth to trap the oil in the closing pocket between the tooth tip and root, causing excessive power loss in the drive.

Results and Discussion

Analytical Results

The equations described in the previous section were computerized, and some of the important parameters were selected for a parametric study, the results of which are reported below.

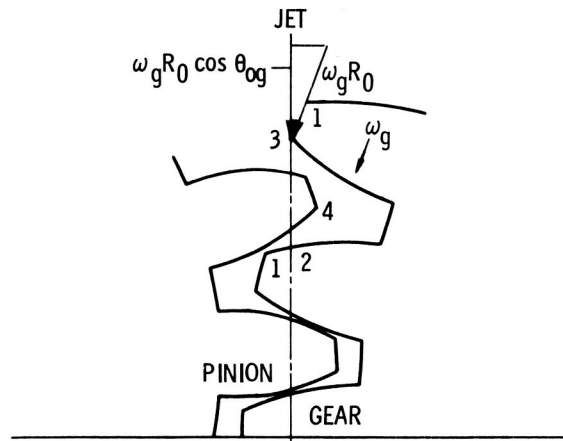


Figure 10

Figure 11 is a plot of the nondimensional impingement depth γ versus the nondimensional jet velocity v_j/v , which shows, as would be expected, a general increase in impingement depth as the jet velocity is increased. This computer study was made using the NASA test gears. These gears have 28 teeth and a gear ratio $m_g = 1.0$. Thus, the impingement depth for the pinion and gear is identical (fig. 11). This, of course, would not be so for ratios other than 1.0. It will be noticed, even at fairly substantial jet velocities such as $v_j/v = 2.0$, that the impingement depth down the profile of the gear tooth is still unimpressive.

Figure 12 shows in general what happens to the impingement depth if the number of teeth in the pinion is changed. The gear and pinion impingement depths are the same and fairly small when the gear ratio is equal to 1.0. If the gear ratio is increased to 2.0 (upper curve of fig. 12), the higher ratio provides a deeper impingement depth γ_g on the gear only. The pinion tooth is missed and does not block the jet to the gear tooth.

The above explanation leads to a more careful examination of the effects of gear ratio on the impingement depth of the pinion and gear, respectively. Figure 13 provides this kind of information for the present example. The 28-tooth pinion is held constant while varying the number of teeth on

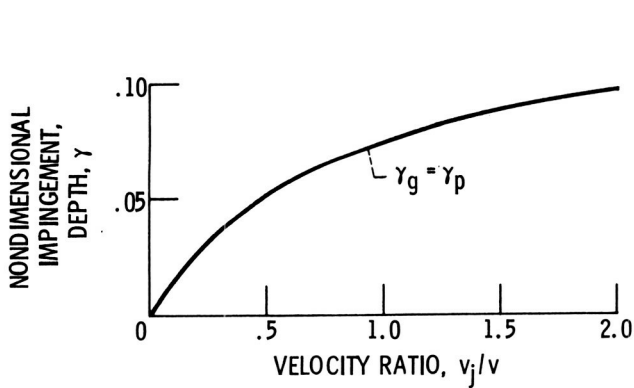


Figure 11. - Velocity ratio as function of nondimensional impingement depth. Speed, 3600 rpm; jet pressure, 17×10^4 Pa (25 psi); $N_p = 28$; $m_g = 1$.

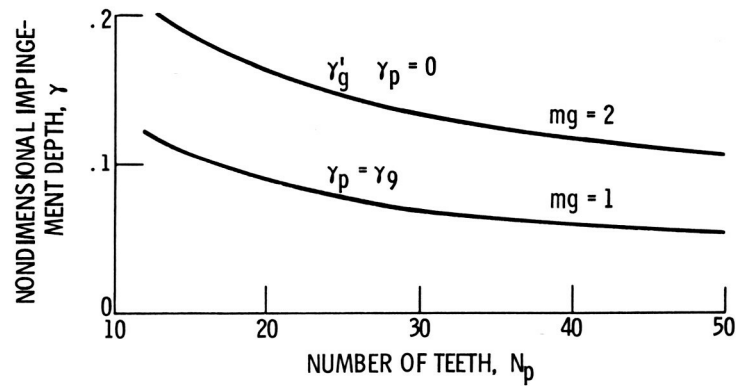


Figure 12. - Number of pinion teeth as function of nondimensional impingement depth. Speed, 3600 rpm; jet pressure, 17×10^4 Pa (25 psi); $v_j/v = 1$

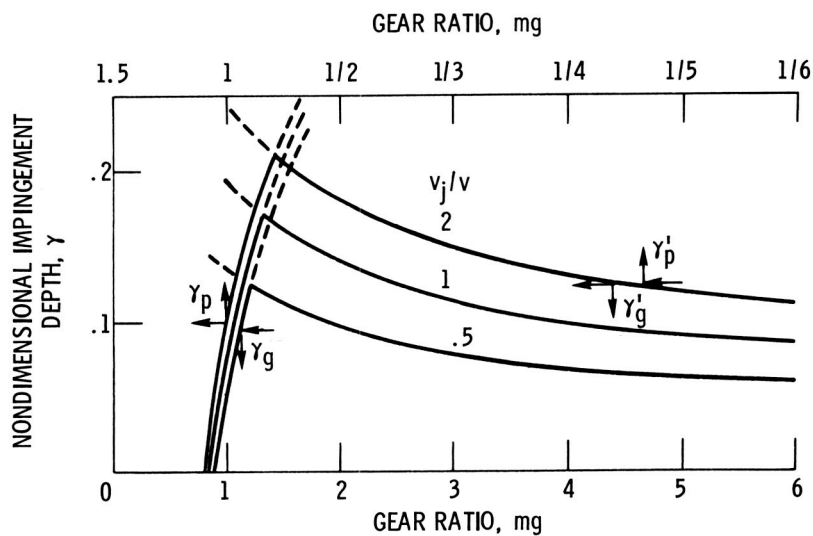


Figure 13. - Gear ratio as function of nondimensional impingement depth. Speed, 3600 rpm; jet pressure, 17×10^4 Pa (25 psi); $N_p = 28$.

the gear to determine what effect this would have on the impingement depth. As can be seen in figure 13, for a jet velocity ratio of 0.5 and a gear ratio of 1.114, the profile of this pinion is no longer impinged by the jet. Only the top land is covered by direct impingement up to a ratio of about 1.25, at which point the leading tooth of the gear begins blocking the trailing tooth. Thus, at gear ratios above about 1.25, when $v_j/v = 0.5$, the impingement depth ratio γ_g will be less than about 0.12 and will drop to 0.04 above a gear ratio of 10. As the jet velocity ratio is increased, the gear receives a somewhat greater depth of impingement. This general trend is shown in figure 13 where the jet velocity was increased to 1.0 and 2.0, respectively. The important thing to note in figure 13 is that the pinion tooth profile is not impinged on directly for speed reducers with ratios above about 1.11 or 1.23, depending on the jet velocity ratio. Gear impingement depth is also limited by leading tooth blocking at ratios above about 1.25 or 1.5.

There is a splash after tooth impingement even when the impingement is only on the top land of a pinion or gear. However, this splash cannot be depended on for the cooling function. It may be useful to point out here that ratios above 1.0 are considered to be speed decreaseers (or reducers), whereas ratios below 1.0 are intended to be interpreted here as speed increaseers (where the gear is the driver). In this particular case the γ_p and the γ_g curves are reversed. The figure 13 curve labeled γ_p and γ_g is therefore plotted to gear ratios less than one so that the curves can be examined in detail for gear increaseers and decreaseers, respectively. Figures 2 to 13 do a reasonably good job of showing the importance of proper location and pointing of the jet nozzle. As can be seen, if the nozzle is pointed slightly off the pitch line, the impingement depth can be severely reduced on one of the members. This results in a great advantage to the other member of the mesh and affects the heat balance between gears.

From a practical standpoint, many gears can be cooled quite adequately with impingement principally on the top land of the gear, except in the case of modified pinions with top lands of very narrow width. In such cases it may be important to position the jet so that the impingement down the profile of the pinion is favored over the gear in such a manner as to balance the cooling on the pinion and gear.

Example

Find the impingement depth on the driven gear using the NASA gear at 3600 rpm and 17.25×10^4 Pa (25 psig) oil pressure, $r_o = 0.0476$ m (1.875 in.), $r = 0.144$ m (1.75 in.), $B_p = B_g = 0$, $N_p = 28 = N_g$, $P = 8$, and $\varphi = 20^\circ$ using equations (25) to (33):

$$\cos^{-1} \frac{r}{r_o} = \cos^{-1} \frac{1.75}{1.875} = 0.3672 \text{ rad}$$

$$\varphi_{op} = \cos^{-1} \frac{r_b}{r_o} = \cos^{-1} \frac{1.644}{1.875} = 0.501117 \text{ rad}$$

$$\text{inv } \varphi_{op} = \tan \varphi_{op} - \text{arc } \varphi_{op} = 0.046637 \text{ rad}$$

$$\text{inv } \varphi = \tan 20 - \text{arc } 20 = 0.0149 \text{ rad}$$

$$\frac{\pi}{N_p} = 0.1122 \text{ rad}$$

$$\theta_{pr} = 0.3672 - 0.046637 + 0.0149 - 0.1122 = 0.22326 \text{ rad} \quad (25)$$

$$\theta_{g2} = 0.22326/1 + 0.1122 - 0 + 0.0149 = 0.35036 \text{ rad} \quad (26)$$

Try $L_g = 0.0156$ m (0.6147 in.) for iteration,

$$\theta_{g4} = \cos^{-1} \frac{1.75 \cos 20}{(1.75^2 + 0.6147^2)^{1/2}} = 0.48044 \text{ rad} \quad (30)$$

$$v_j = 156 \sqrt{25} = 19.8 \text{ m/sec (780 in/sec)} \quad \omega = 377 \text{ rad/sec}$$

$$\text{inv } \theta_{g4} = \tan \theta_{g4} - \text{arc } \theta_{g4} = 0.04085 \text{ rad}$$

$$\theta_{g3} = \tan^{-1} 0.6147/1.75 + 0.4085 = 0.3786 \text{ rad} \quad (31)$$

Test:

$$\frac{(0.3786 - 0.35036)}{377} = \frac{(1.875^2 - 1.75^2)^{1/2} - 0.6147}{780}$$

$$0.000075 = 0.000075$$

$$H_g = 1.875 - [(1.75)^2 + (0.6147)^2]^{1/2} = 0.0005 \text{ m (0.0202 in.)} \quad (33)$$

Experimental Results

Figure 14(a) shows the oil jet just after it clears the gear tooth with the pinion tooth still blocking the following gear tooth. In figure 14(b) the jet has cleared the pinion tooth and is impinging on the gear tooth at the maximum depth for this condition. The test conditions for figure 14 was 3600 rpm, which gives a v of 16.7 m/sec (660 in/sec) and an oil-jet pressure of 8.3×10^4 Pa (12 psi) for a calculated v_j of 13.7 m/sec (540 in/sec) and a v_j/v of 0.82. The impingement depth for these test conditions is 0.043 cm (0.017 in.). The experimental depth (fig. 14(b), while difficult to measure with precision, agrees with the calculated impingement depth.

In figure 15 the test conditions were 3600 rpm, which gives a v of 16.7 (660 in/sec) and an oil-jet pressure of 17.25×10^4 Pa (25 psig), for a v_j of 20 m/sec (780 in/sec). This gives a v_j/v of 1.18. The calculated impingement depth for these test conditions is 0.05 cm (0.02 in.). Figure 15(a) shows the jet at the tip of the leading gear tooth just before it starts toward the pinion tooth. In figure 15(b) the



Figure 14. - Oil jet impingement depth, out of mesh condition. Speed, 3600 rpm; jet pressure, 8.3×10^4 Pa (12 psi).

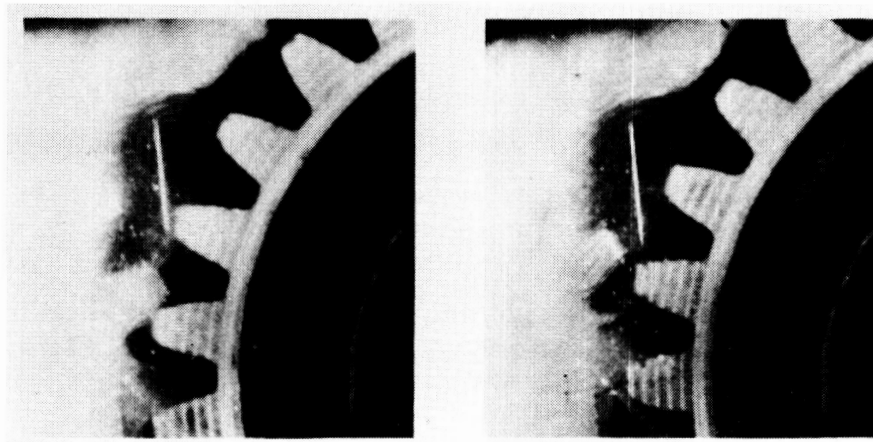


Figure 15. - Oil jet impingement depth, out of mesh condition. Speed, 3600 rpm; jet pressure, 17.25×10^4 Pa (25 psi).

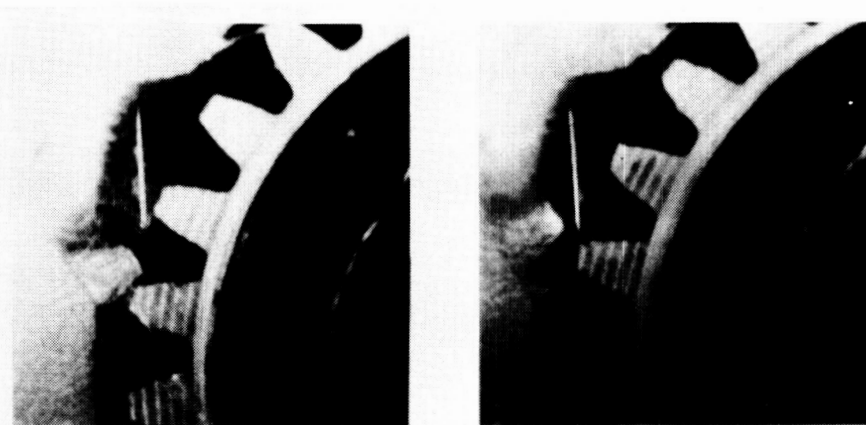


Figure 16. - Oil jet impingement depth, out of mesh condition. Speed, 5000 rpm; jet pressure, 13.8×10^4 Pa (20 psi).

pinion tooth has passed the oil jet, and the jet is about to impact the gear tooth at an experimental impingement depth close to the calculated depth.

Figure 16 shows two high-speed camera picture frames taken at 2300 frames per second with the gears running at 5000 rpm for a v_p of 23.4 m/sec (920 in/sec). This camera and gear speed give a picture for each tooth space movement of the gear. The oil-jet pressure was 13.8×10^4 Pa (20 psig) giving a v_j of 17.8 m/sec (700 in/sec). The v_j/v for these conditions is 0.76 giving a calculated impingement depth of 0.04 cm (0.016 in.). In figure 16(a) the oil jet has just passed the tip of the gear tooth and the pinion tooth is still between the jet and the following gear tooth. In figure 16(b), the oil jet has cleared the pinion tooth tip and is impacting the gear tooth at near the calculated impingement depth.

Summary Of Results

An analysis was conducted for oil-jet lubrication on the disengaging side of a gear mesh. Results of the analysis were computerized and used to determine the oil-jet impingement depth for several gear ratios and oil-jet to pitch-line velocity ratios. An experimental program was conducted on the NASA gear test rig using high-speed photography to experimentally determine the oil-jet

impingement depth on the disengaging side of mesh.

The following results were obtained:

1. Impingement depth reaches a maximum at gear ratios near 1.5 where chopping by the leading gear tooth limits the impingement depth.
2. The pinion impingement depth is zero above a gear ratio of 1.172 for an oil-jet to pitch-line velocity ratio of 1.0 and is similar for other velocity ratios.
3. The impingement depth for gear and pinion are equal and approximately one half the maximum at a gear ratio of 1.0.
4. Impingement depth on either the gear or pinion may be improved by relocating the jet away from the pitch line or by changing the jet angle.
5. Results of the analysis were verified by experimental results using a high-speed camera and a well lighted oil jet.

References

1. McCain, J. W.; and Alsandor, E.: Analytical Aspects of Gear Lubrication on the Disengaging Side. Trans. ASLE, vol. 9, Apr. 1966, pp. 202-211.
2. Akin, L. S.; Mross, J. J.; and Townsend, D. P.: Study of Lubricant Jet Flow Phenomena in Spur Gears. J. Lubr. Technol., vol. 97, no. 2, Apr. 1975, pp. 283-288.
3. Akin, L. S.; and Mross, J. J.: Theory for the Effect of Windage on the Lubricant Flow in the Tooth Spaces of Spur Gears. J. Eng. Ind., vol. 97, Nov. 1975, pp. 1266-1273.
4. Fujita, K.; Obata, F.; and Matsuo, K.: Instantaneous Behavior of Lubricating Oil Supplied Onto the Tooth Flanks and Its Influence on the Scoring Resistance of Spur Gears. J. Eng. Ind., vol. 98, no. 2, May 1976, pp. 635-643.
5. Townsend, D. P.; and Zaretsky, E. V.: A Life Study of AISI M-50 and Super Nitralloy Spur Gears with and without Tip Relief. J. Lubr. Technol., vol. 96, no. 4, Oct. 1974, pp. 583-590.